

Assessment of bacterial biofilm on stainless steel by hyperspectral fluorescence imaging

Won Jun · Moon S. Kim · Kangjin Lee ·
Patricia Millner · Kuanglin Chao

Received: 20 November 2008 / Accepted: 5 January 2009 / Published online: 30 January 2009
© USDA, Agricultural Research Service 2009

Abstract Hyperspectral fluorescence imaging techniques were investigated for detection of two genera of microbial biofilms on stainless steel material which is commonly used to manufacture food processing equipment. Stainless steel coupons were deposited in nonpathogenic *E. coli* O157:H7 and *Salmonella* cultures, prepared using M9 minimal medium with casamino acids (M9C), for 6 days at 37 °C. Hyperspectral fluorescence emission images of the biofilm formations on the stainless coupons were acquired from 416 to 700 nm with the use of ultraviolet-A (320–400 nm) excitation. In general, emission peaks for both bacteria were observed in the blue region at approximately 480 nm and thus provided the highest contrast between the biofilms and background stainless steel coupons. A simple thresholding of the 480 nm image showed significantly larger biofilm regions for *E. coli* O157:H7 than for *Salmonella*. Viable cell counts suggested that *Salmonella* formed significantly higher density biofilm regions than *E. coli* O157:H7 in M9C medium. On the basis of principal component analysis (PCA) of the hyperspectral fluorescence images, the second principal component image exhibited the most distinguishable morphological

differences for the concentrated biofilm formations between *E. coli* and *Salmonella*. *E. coli* formed granular aggregates of biofilms above the medium on stainless steel while *Salmonella* formed dense biofilm in the medium-air interface region (pellicle). This investigation demonstrated the feasibility of implementing fluorescence imaging techniques to rapidly screen large surface areas of food processing equipment for bacterial contamination.

Keywords Biofilm · Bacteria · Hyperspectral imaging · Fluorescence

Introduction

Escherichia coli O157:H7, *Salmonella* spp., and other human pathogens such as *Staphylococcus aureus* and *Listeria monocytogenes* are known to attach to food surfaces and to a variety of abiotic surfaces such as stainless steel, plastic, glass, and cement [1], and to form biofilms which can act as harbor sites for micro-organisms on food and equipment surfaces. Biofilms have been associated with over 80% of human infections, according to the U.S. National Institutes of Health [2]. In general, bacteria exist in two different types of populations: as single planktonic cells, and as structured, multicellular communities of bacteria embedded within a matrix of extracellular polymeric substances (EPS) known as bacterial biofilms [3]. Individual cells from the planktonic condition attach to a surface as a first step for biofilm formation and then secrete a polysaccharide-like substance that adheres the cells to the surface and to one another. Then, the organisms can establish a community of biofilms. This can cause cross-contamination of foods and food processing environments through cell sloughing [4]. The formation of biofilm

Company and product names are used for clarity and do not imply any endorsement by USDA to the exclusion of other comparable products.

W. Jun · M. S. Kim (✉) · P. Millner · K. Chao
Food Safety Laboratory, Animal and Natural Resources Institute,
U.S. Department of Agriculture, Agricultural Research Service,
Powder Mill Rd. Bldg 303, BARC-East, Beltsville, MD 20705,
USA
e-mail: moon.kim@ars.usda.gov

K. Lee
National Institute of Agricultural Engineering, Rural
Development Administration, 249 Seodun-dong, Gwonson-Gu,
Suwon 441-100, Republic of Korea

enhances the activity of microorganisms and provides for them a protective shield that reduces their susceptibility to environmental stress such as desiccation, starvation or heavy metals. Bacteria attached to surfaces also show greater resistance to disinfection [5]. These are significant concerns for the food processing industry since the biofilm-associated microorganisms can raise food safety and public health risks, and also increase economic losses incurred due to product spoilage [6, 7]. Biofilm contamination on foods and food processing equipment suggests that sanitation procedures during food processing operations may be inadequate. Hence, there is a need to develop rapid and nondestructive biofilm detection methods for more effective cleaning and sanitizing procedures and to prevent potential cross-contamination in food processing environments.

Various methods have been developed and are used for the detection of microbial targets. Some popular methods for detecting bacterial contamination, such as crystal violet-based assay, colony counting methods, polymerase chain reaction (PCR), real-time-PCR, and immunology-based systems, are labor-intensive, time-consuming, and still require trained personnel [8]. Interest in the development of rapid detection biosensors for microbial contamination has been growing in recent years. Biosensors can be classified into the following groups based on signal transduction method: optical, electrochemical, thermometric, piezoelectric, magnetic, or micromechanical. Optical biosensors using fluorescence methods have been developed to detect different pathogens [9]. Development of optical biosensors is generally based on measuring the differences in light absorption of chemical reactant and product substances, or measuring the light output produced by a luminescent process. Biosensor-based techniques allow for a sensitive and specific assessment to detect low concentrations of target microbes, without the involvement of chemistry-based analytical procedures.

Despite their high sensitivity and specificity for detecting particular microbial contaminants, these biosensors may not be well-suited for screening relatively large surface regions, such as food processing equipment surfaces, for bacterial harbor sites. A method and technology capable of rapidly scanning relatively large surface areas for assessing potential bacterial harborage site may effectively complement recent developments in biosensor technologies.

It is feasible, owing to the advancements of low-light sensitive opto-electronic sensors, to rapidly measure auto-fluorescence of materials with relatively low fluorescence yield [10]. For fluorescence imaging applications in large-scale sensing, researchers at the Agricultural Research Service (ARS), Food Safety Laboratory have developed several platforms that monitor the quality and safety attributes of a variety of agricultural food products [10–14].

Most recently, we developed a line-scan (push broom) hyperspectral imaging system that is capable of reflectance and fluorescence measurements.

The goal of this research was to evaluate the potential of hyperspectral fluorescence imaging techniques for screening and detection of bacterial biofilms on stainless steel surfaces. Imaging techniques add the advantage of spatial assessment capabilities (i.e., pattern recognition). We also investigated the feasibility of using hyperspectral fluorescence imaging in conjunction with principal component analysis to potentially classify the different bacteria based on spectral and spatial features. Because a number of biological materials emit fluorescence, biofilms in this study were grown in a bacterial growth medium exhibiting minimal auto-fluorescence, to mitigate the effect of the medium and to examine the auto-fluorescence emanating from the microbial biofilms.

Materials and methods

Culture preparation

Nonpathogenic bacteria, *E. coli* O157:H7 strain 3704 and *Salmonella enterica* typhimurium ATCC 53648, were used in this investigation. To prepare inocula, *E. coli* and *Salmonella* were first surface-plated on tryptic soy agar (TSA; Difco, Sparks, MD, USA) plates and incubated at 37 °C for 24 h. For each strain, single colonies were inoculated into 10 ml of M9 medium with casamino acids (Difco Laboratories, Detroit, MI) and incubated at 37 °C for 24 h. M9 medium with casamino acids (M9C) was prepared as described by ATCC medium 1281 (www.atcc.org) and included, per liter: 200 mL of M9 minimal salts, 5×; Casamino acids 5 g; Na₂HPO₄ 6 g; KH₂PO₄ 3 g; NaCl 0.5 g; NH₄Cl 1 g; 1 mL of 1 M MgSO₄; 10 mL 1 mg/mL thiamine; 1 mL CaCl₂ (0.1 M).

Biofilm formation experiments

A batch of 75 µL of 24 h grown cultures was inoculated into 15 mL of M9C in each of 6 50-mL falcon conical tubes, and 6 sterile stainless steel coupons (Type 304, #4 finish, 2 by 5 cm) were prepared as described by Ryu et al. [15]. Each coupon was deposited into one tube such that approximately half of the coupon was submerged in the culture. Samples were incubated at 37 °C in static condition for 6 days, and hyperspectral fluorescence images of the sample coupons were acquired on the 6th day following the *E. coli* and *Salmonella* inoculations. Note that because of the nutrient limitation of the M9C medium, spent medium was replaced with fresh M9C medium every 48 h. We also predetermined that 6-day incubation of the

coupons was ideal for fluorescence imaging of the biofilm samples formed in the nutrient-limited medium.

To enumerate biofilm cells, each coupon was transferred to a 50-mL tube containing 30 mL of PBS and 3 g of sterile glass beads. The tube containing PBS, coupon, and glass beads was vortexed at maximum speed for 1 min to dislodge cells from the biofilms. Immediately after vortexing, samples serially diluted in PBS were surface plated on TSA and incubated at 37 °C for 24 h. Colonies were counted and populations (CFU/mL) remaining on stainless steel coupons before and after hyperspectral fluorescence imaging were calculated. The number of detached biofilm cells was reported as CFU/cm². The experiment was replicated two times.

Hyperspectral fluorescence imaging system

The hyperspectral imaging system (Fig. 1) utilizes an electron-multiplying charge-coupled-device (EMCCD: MegaLuca R, ANDOR Technology, South Windsor, CT, USA). The EMCCD consists of a 1002 × 1004 array of pixels (each 8 × 8 μm²) and is thermoelectrically cooled to −20 °C. It operates at a maximum of 12.5 MHz pixel-readout rate and image data is digitized in 14-bit. An imaging spectrograph (VNIR Concentric Imaging Spectrograph, Headwall photonics, Fitchburg, Massachusetts) and a C-mount object lens (F1.9 35 mm compact lens, Schneider Optics, Hauppauge, NY, USA) are attached to the EMCCD. The IFOV (instantaneous field of view) is limited to a thin line by the spectrograph aperture slit (25 μm). Through the slit, light from the IFOV line is dispersed by a concentric grating and projected onto the EMCCD. Therefore, for each line-scan, a two-dimensional (spatial and spectral) image is created with the spatial

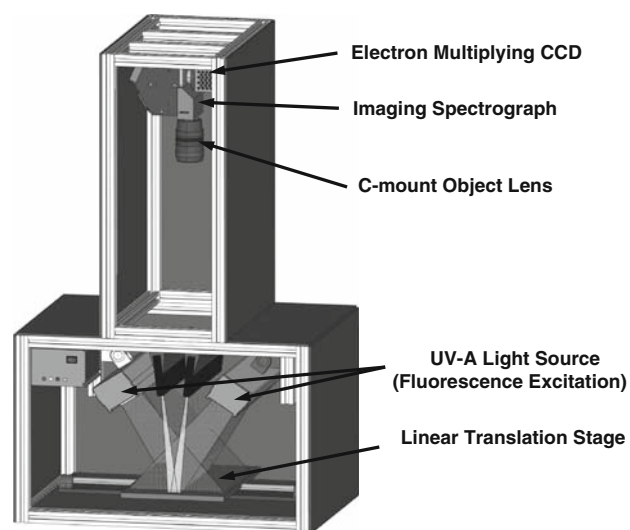


Fig. 1 Hyperspectral fluorescence imaging system

dimension along the horizontal axis and the spectral dimension along the vertical axis of the EMCCD. For fluorescence imaging, the sample illumination is provided by a pair of UV-A lamps (365 nm, EN-280 L/12, Spectronics Corp., Westbury, NY, USA).

For hyperspectral fluorescence imaging, the vertical pixels (spectral) were binned by 6, resulting in a total of 60 channels spanning from 416 to 700 nm with a spectral increment of approximately 4.79 nm per channel. The horizontal pixels were binned by 2 (=502 pixels) to result in the spatial resolution of approximately 0.25 mm, and the line scans were acquired at increments of 0.5 mm. For each experiment replicate, a set of sample images consisted of a total of 14 coupons: 6 *E. coli* and 6 *Salmonella* coupons, each arranged in 2 rows by 3 columns, and two M9C control coupons.

With the use of SDK (Software Development Kit) provided by the EMCCD manufacturer, interface software for the imaging system control and data acquisition was developed on a MS Windows Visual Basic (Version 6.0) platform. We also developed image processing and analysis software using a MS Windows Visual Basic platform. The biofilm formation areas on stainless steel surface were determined by a simple thresholding method. Total numbers of pixels for *E. coli* and *Salmonella* biofilm formation area on each coupon were tabulated for comparisons.

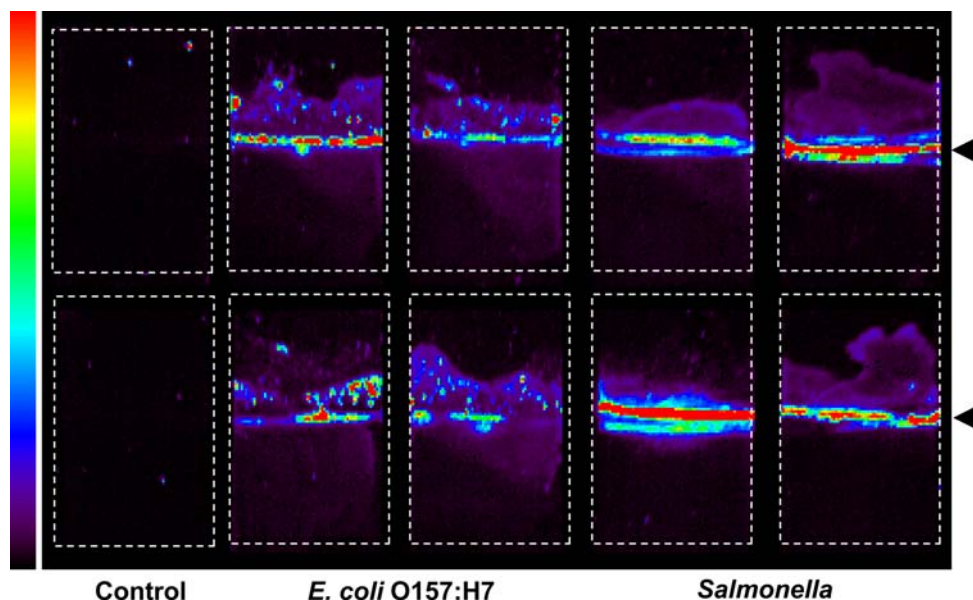
Principal component analysis (PCA) of the entire spectral region (60 channels) of the sample hyperspectral fluorescence images was performed using ENVI (Environment for Visualizing Images, Version 3.2, Research Systems Inc., CO). Each principal component (PC) image consists of a linear sum of responses at individual pixels weighted by corresponding spectral weighing coefficients (eigenvectors). The PC images are ordered by their variance sizes, and may allow us to examine the hyperspectral responses of the samples in a reduced dimension (dimensionality reduction) for the potential classification of bacterial biofilm by genera.

Results

Hyperspectral fluorescence imaging for detection of biofilm contamination

A representative, pseudo-color fluorescence image of coupons with M9C medium only, followed by coupons with biofilm formations of *E. coli* and *Salmonella* grown in M9C minimal medium at near 480 nm, are shown in Fig. 2. Note that the dotted outlines for individual coupons were added for clarity. Coupons with only the M9C medium control treatment exhibited minimal fluorescence. For the other coupons, biofilms were formed not only in the

Fig. 2 Representative fluorescence emission image of sample coupons with biofilms formed by *E. coli* O157:H7 and *Salmonella* at 480 nm, acquired with the hyperspectral imaging system. The arrowheads indicate the medium fill lines. Approximately half of each coupon was submerged in a 50-mL tube containing 15 mL M9C broth for 6 days at 37 °C without shaking. Small spots on the control coupons were due to dust particles settling during the measurement



medium, but also on and above the medium-air interface, indicating that cells migrated above the submersion level of the coupons in the M9C medium and produced biofilms. The *E. coli* image showed aggregates of granule-like spots above the culture medium. The *Salmonella* image revealed that more concentrated biofilms were developed on the air-medium interface region (pellicle) than *E. coli*.

Biofilms formed by *E. coli* O157:H7 and *Salmonella* showed a range of fluorescence emission intensities. However, *E. coli* O157:H7 and *Salmonella* showed similar spectral responses throughout the emission range under investigation, from 416 to 700 nm (Fig. 3). Each spectrum

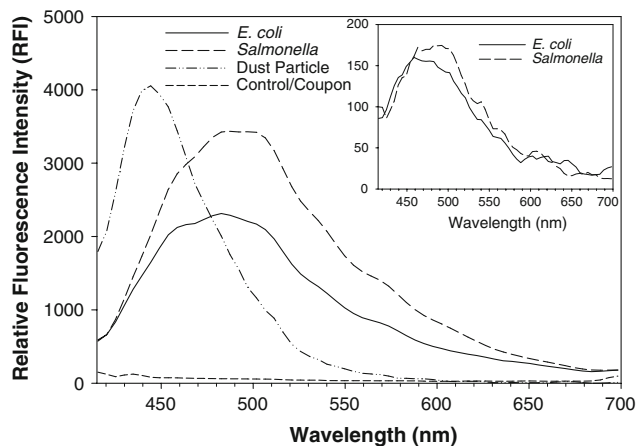


Fig. 3 Representative fluorescence spectra of *E. coli* O157:H7 and *Salmonella* biofilms formed on stainless steel coupons in M9C medium. Spectra were extracted from the hyperspectral image data where each spectrum represents a mean obtained from 6 coupons in the medium fill-line regions. Control indicates medium-only spots on stainless steel coupons. A representative fluorescence spectrum of dust particles is also shown

represents an average of 6 individual spectra, each obtained from a minimum of 2×2 pixel region of interest (ROI) near the air-medium interface portion of the coupons with relatively high fluorescence emission intensities. The smaller graph (Fig. 3, inset upper right) shows representative spectra of the thin biofilm growth regions.

In general, fluorescence spectral data revealed that emission maxima occurred at around 480 nm for both bacterial biofilms. The control coupons in Fig. 2 exhibited a few bright small spots which were due to the dust particles as evident by a mean spectrum extracted from these spots with the emission peak at around 430 nm (Fig. 3). It was also found that some dust particles settled on the biofilm regions of both *E. coli* O157:H7 and *Salmonella* during the hyperspectral measurements.

The microbial biofilms grown in M9C minimal medium showed relatively higher fluorescence emission intensities with emission peaks in the blue-green regions compared to the control treatments of M9C medium on stainless steel coupon. Thus, biofilms can be discriminated from the stainless steel/M9C medium background and the biofilm regions can be quantified using a single band fluorescence emission band. In this investigation, a simple global thresholding method with a threshold value, determined by the following method, was used to quantify the biofilm regions. Figure 4 shows the histogram of the 480 nm image for the background regions (M9C medium and coupons) and for the thin biofilm regions. Apparently, the fluorescence intensities of the background and biofilm regions overlapped as the result of relatively low fluorescence emission emanating from the very thin biofilm formations. The fluorescence intensity frequencies peaked at approximately 50 and 200 for the background and thin

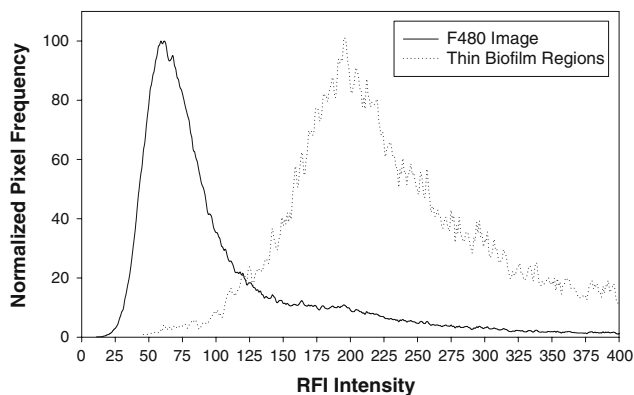
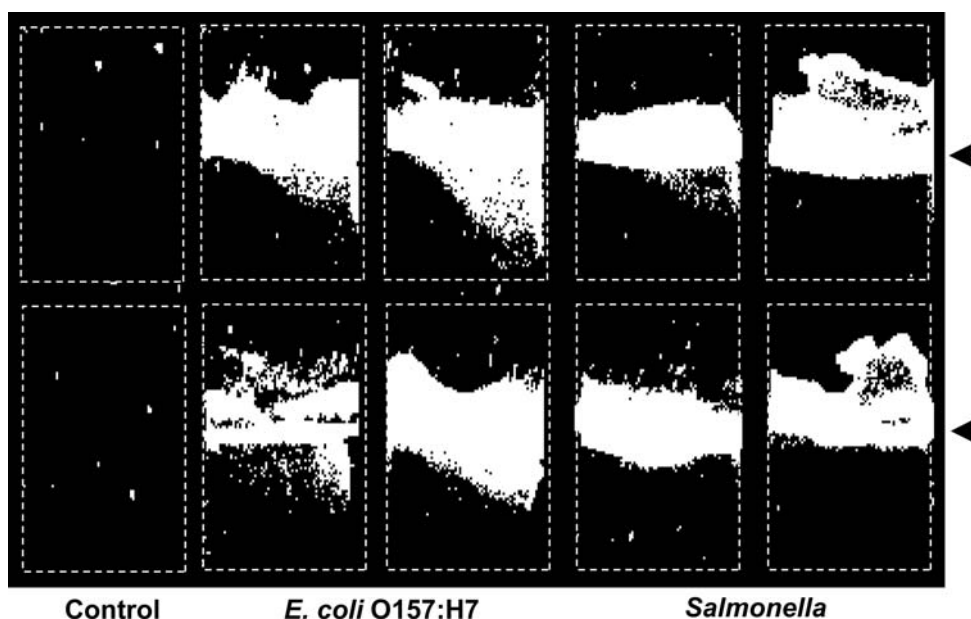


Fig. 4 Pixel intensity-frequency histogram of the 480 nm fluorescence image for the F480 image background and for the thin biofilm regions

biofilm regions, respectively. The intermediate value of 125 for the two overlapping histogram intensity distribution was chosen as the threshold value to quantify the biofilm formation regions.

The resultant binary image for biofilm formation regions upon applying a global thresholding value of 125 is shown in Fig. 5. The total numbers of biofilm region pixels for *E. coli* O157:H7 and *Salmonella* were 2893 (± 262.3 , standard error) and 2154 (± 165.1 , standard error), respectively, and were significantly different. More thinly spread regions of biofilm formations below the medium fill line were observed for *E. coli* than for *Salmonella*. These results demonstrated that a single waveband fluorescence image may allow detection of biofilm contamination on stainless steel surfaces.

Fig. 5 Binary image showing biofilm-covered regions on coupons, determined by applying global thresholding to the 480 nm fluorescence image. Small spots on the control coupons (false-positives) were due to dust particles settling during measurement. The arrowheads indicate the medium fill lines



Principal component analysis

The blue fluorescence image at 480 nm showed a subtle difference in biofilm formation pattern between the two genera. The formation patterns between *E. coli* and *Salmonella* may be differentiated with additional image processing. Principal components analysis (PCA) was applied to hyperspectral fluorescence image data to reduce the spectral data to a lower dimensional factor space [16]. Note that PCA has been used for both classification and dimensionality reduction tools.

Figure 6 shows the first three PC images (a, b, c) for the stainless steel coupons with the control treatment (column 1 on left), biofilms of *E. coli* (columns 2 and 3) and *Salmonella* (columns 4 and 5). The first PC (PC1) explains the largest variance of fluorescence emission in the class followed by the subsequent PCs. Each of the first few PC images failed to classify *E. coli* and *Salmonella* as two distinct classes. This suggests that the spectral variations for the thin and concentrated biofilm regions were not unique to either of the two genera and that the spectral responses for both genera were very similar. However, PC1 and PC2 images showed distinguishable spatial growth features for the two genera with high fluorescence intensity (concentrated growth regions). Note that PC1 shows biofilm areas as brighter color on a darker background while PC2 shows biofilm growth areas as darker spots on a gray background. The PC2 image particularly enhanced unique spatial features of the concentrated biofilm growths for both bacteria. Note that sparsely scattered, false positives due to dust particles as black spots were observed on each coupon. *Salmonella* formed extensive biofilm formations

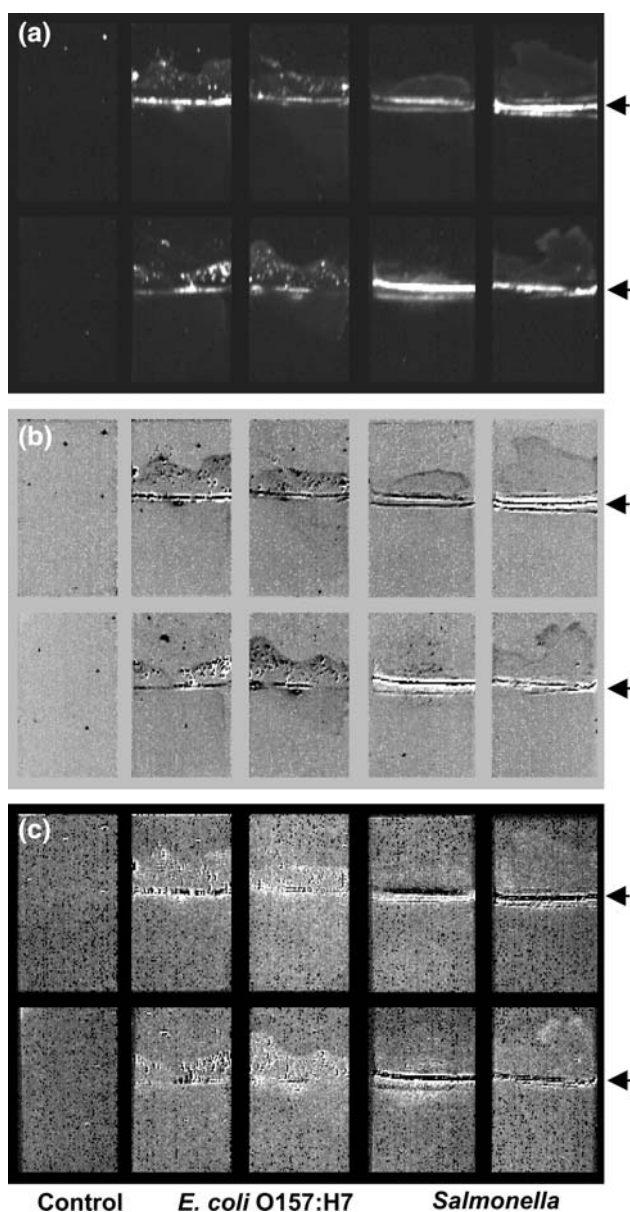


Fig. 6 The first (a), second (b), and third (c) principal component (PC) score images obtained from the hyperspectral fluorescence images of control medium, and *E. coli* and *Salmonella* biofilms on stainless steel coupons. The arrowheads indicate the medium fill lines

along the medium fill lines, whereas concentrated *E. coli* growth was scattered above the medium fill lines. A binary image of the PC2 for the darker regions was created using a simple thresholding method (Fig. 7). The result highlights the concentrated biofilm formations and clearly exhibits the concentrated growth pattern difference between the two genera suggesting that the two organisms had different preferential growth environments. The PCA provided enhancement of the spatial features such that biofilm formations on the stainless surfaces, produced by two different organisms, can be differentiated.

Quantification of cells in the biofilm

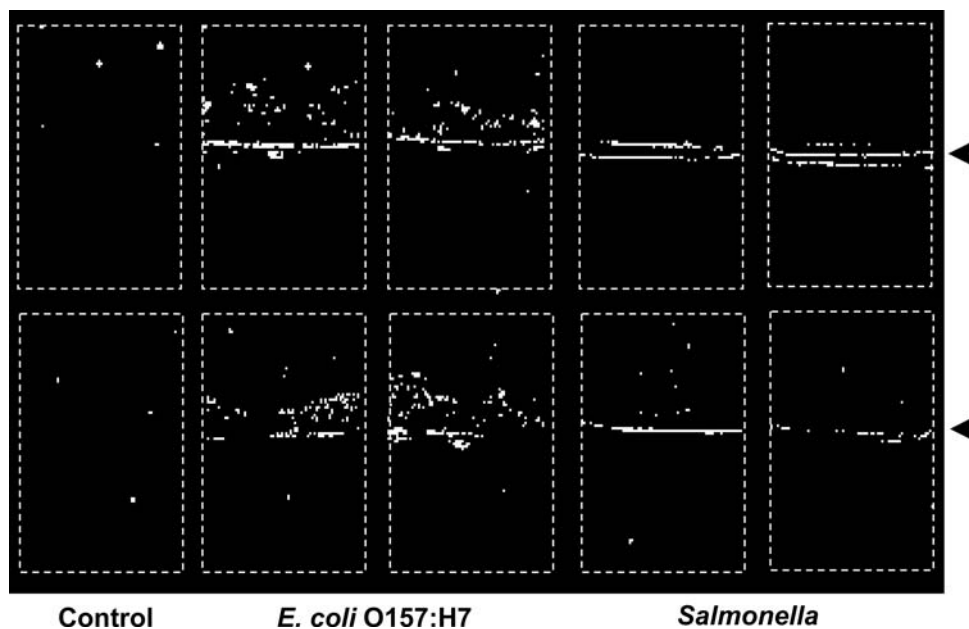
By breaking up the biofilms with glass beads and dislodging cells, viable plate counts could be acquired to determine the number of bacteria growing on the stainless steel coupons. The results are expressed as the population of CFU cm^{-2} of each bacterium (Fig. 8). For 6-day-old cultures, *E. coli* formed biofilm on the stainless steel with a cell density of 3×10^7 CFU cm^{-2} while *Salmonella* formed biofilm with a cell density of 1.2×10^8 CFU cm^{-2} . Obtained in 2 independent experiments ($n = 6$), the biofilm *Salmonella* population was slightly higher than the biofilm *E. coli* population (~ 4 fold). The cells were quantified again after hyperspectral fluorescence imaging since exposure to UV and dryness causes cells to die. A 1-log reduction was shown by the post-imaging *E. coli* counts of 2×10^6 CFU cm^{-2} , with about 6% survival. In contrast, about 35% of the cells in the *Salmonella* biofilm survived, showing only a 4-fold reduction as a result of the exposure to UV and dryness. Thus, the *Salmonella* biofilm population was shown to be slightly more tolerant than the *E. coli* biofilm population. Planktonic cells of each bacterium were also quantified for a 6-day-old M9C culture after the removal of stainless steel coupons from the cultures. The results for *E. coli* and *Salmonella* cells were both 2×10^9 CFU/ml (data not shown). The ability of *Salmonella* to survive stress conditions, in this case UV and dryness, compared with *E. coli*, may be due to either *Salmonella* having been present in slightly higher numbers than *E. coli* in the biofilm or to several other factors involving cellular attachment.

Discussion

Food borne illness associated with bacterial contamination is a significant public health concern. The illness has been mainly linked with biofilms formed by food-borne pathogens such as *E. coli* O157:H7, *Salmonella* spp., and *Listeria monocytogenes*. Detection of microbial biofilms in food processing environments could greatly reduce food safety risks. Hyperspectral fluorescence imaging methods were investigated for detection of microbial contamination (biofilm) on stainless steel surfaces, typical of the material used for food processing equipments.

The fluorescence imaging of biofilms demonstrated the visualization and quantification of growth regions and assessment of growth patterns for two genera of bacteria. This investigation was one of the first studies to show morphology growth features of biofilm formation using hyperspectral imaging techniques. Relatively concentrated biofilms of *E. coli* exhibited a pattern with aggregates of granule-like spots above the surface of the liquid culture

Fig. 7 Binary image showing concentrated biofilm growth regions on coupons, as determined by the second PC score image of the hyperspectral fluorescence image data. *Small spots* on the control coupons (false-positives) were due to dust particles settling during measurement. The *arrowheads* indicate the medium fill lines



medium on stainless steel coupons (Figs. 2, 6). However, *Salmonella* formed clump-shaped biofilm around the medium-air interface (pellicle). There is much interest in that colonization of the interface between air and liquid where aerobic or facultative aerobic bacteria may have an advantage during a medium surface colonization [17]. Most bacteria propagated in liquid culture grow dispersed, sink to the bottom, form aggregates, or pellicles after static growth in broth. However, several bacteria, such as *Salmonella enterica* serovars, *Escherichia coli*, *Pseudomonas fluorescens*, and *Vibrio cholerae*, are capable of colonizing and forming either fragile or rigid pellicles at the air-medium interface [18].

On the basis of fluorescence emission responses of bacterial biofilms in the blue region the spectrum, biofilm formation areas on stainless steel coupons was estimated to be larger for *E. coli* than *Salmonella*. Our plate cell count results showed that biofilm cells of *Salmonella* numbered $\sim 1 \log_{10}$ greater than those of *E. coli* (Fig. 8), suggesting significantly denser biofilm formations on stainless steel coupons compared to *E. coli*. In order to use the fluorescence imaging for quantification of the biofilm cells, fluorescence intensity variations as indicators of cell density may need to be incorporated to potentially estimate the biofilm cell counts. A further investigation is planned.

For this investigation, a growth medium with minimal fluorescence was used. Growth medium composition can have a significant impact on biofilm-forming capability [19]. In addition, a number of other factors may affect the growth and formation of biofilms. Our preliminary investigation showed that the emission spectra from biofilms grown in a nutrient-rich medium exhibited significantly higher fluorescence emissions at also around 480 nm than

those grown in M9C. Further research is needed to correlate the bacterium- and medium-dependent biofilm formation characteristics such as growth area and density, and cell counts. However, the control treatment samples of nutrient-rich medium on stainless steel background exhibited fluorescence emission intensities nearly identical to those of the biofilms under investigation. Therefore, detecting the presence of medium-like substances as a potential harbor site for microbial growth may also be useful as an indirect means to reduce potential food safety risks.

To detect pathogens, biosensors may require a pre-enrichment step to increase the cell counts of the pathogen,

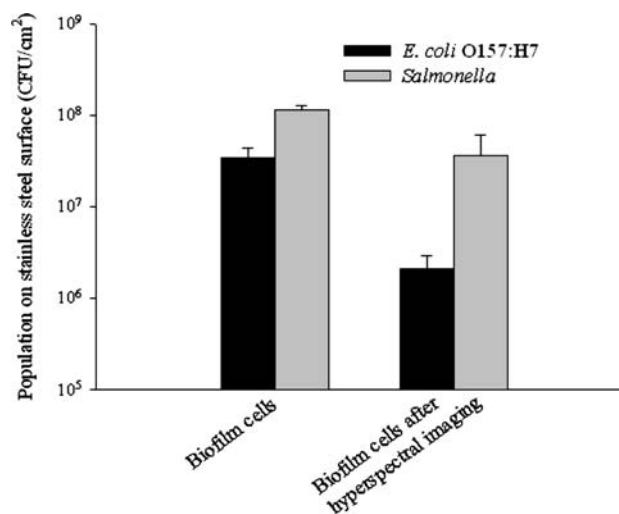


Fig. 8 Biofilm cell counts for *E. coli* O157:H7 (black) and *Salmonella* (gray) recovered from stainless steel surfaces on M9C after 6-day growth at 37 °C. Mean values \pm standard deviations (error bars, $n = 6$) from two independent experiments are shown

to further concentrate the target organism from a large volume of food samples because of the low level presence of pathogens [20]. Taking into consideration the above facts, we can pre-screen surfaces for microbial contamination on food processing equipment with the fluorescence imaging techniques presented in this study. This can compliment the use of biosensors designed to assess specific microbial targets [9, 21]. Our ultimate goal is to develop a handheld portable device that can be used to assist visual sanitation inspection for microbial contamination, such as bacterial biofilm. This device can help address food processing industry concerns regarding microbial contamination occurring on equipment in areas where nutrients can build up and cleaning agents cannot effectively access, or on equipment that is not intended to be routinely disassembled for thorough cleaning. Thus, inspectors can check and identify the suspicious microbial harborage sites with the help of a handheld device before and after the equipment is cleaned and sanitized.

Conclusions

In this paper, we presented a fluorescence imaging method for detection of microbial biofilms on stainless steel coupons. Results show that the fluorescence emission maxima were observed at 480 nm for both *E. coli* O157:H7 and *Salmonella* biofilms on stainless steel surfaces. The 480 nm band can be potentially used to develop a portable imaging device for sanitation monitoring of food processing equipment surfaces. On the basis of principal component analysis (PCA) of the hyperspectral fluorescence images, the second principal component image exhibited the most distinguishable morphological differences between the concentrated biofilm formations of *E. coli* and *Salmonella*. The hyperspectral fluorescence imaging techniques may allow classification of different genera of bacteria. A further investigation with additional genera is planned.

Acknowledgment Authors thank Ms. Diane Chan of the Food Safety Laboratory, ARS, USDA for helping with hyperspectral image collection and reviewing the manuscript.

References

1. B.A. Niemira, *Appl. Environ. Microbiol.* **73**(10), 3239–3244 (2007). doi:[10.1128/AEM.02764-06](https://doi.org/10.1128/AEM.02764-06)
2. M. Kalmokoff, P. Lanthier, T.-L. Tremblay, M. Foss, P.C. Lau, G. Sanders, J. Austin, J. Kelly, C.M. Szymanski, *J. Bacteriol.* **188**(12), 4312–4320 (2006). doi:[10.1128/JB.01975-05](https://doi.org/10.1128/JB.01975-05)
3. R.M. Donlan, J.W. Costerton, *Clin. Microbiol. Rev.* **15**(2), 167–193 (2002). doi:[10.1128/CMR.15.2.167-193.2002](https://doi.org/10.1128/CMR.15.2.167-193.2002)
4. R.A.N. Chmielewski, J.F. Frank, *Compr. Rev. Food Sci. Food Saf.* **2**(1), 22–32 (2003). doi:[10.1111/j.1541-4337.2003.tb00012.x](https://doi.org/10.1111/j.1541-4337.2003.tb00012.x)
5. C. Keevil, *Encyclopedia of Environmental Microbiology*. (Wiley, New York, 2002), pp. 2339–2356
6. B. Carpentier, O. Cerf, *J. Appl. Bacteriol.* **75**(6), 499–511 (1993)
7. C.G. Kumar, S.K. Anand, *Int. J. Food Microbiol.* **42**(1–2), 9–27 (1998). doi:[10.1016/S0168-1605\(98\)00060-9](https://doi.org/10.1016/S0168-1605(98)00060-9)
8. S.S. Branda, A. Vik, L. Friedman, R. Kolter, *Trends Microbiol.* **13**(1), 20–26 (2005). doi:[10.1016/j.tim.2004.11.006](https://doi.org/10.1016/j.tim.2004.11.006)
9. D. Ivnitski, I. Abdel-Hamid, P. Atanasov, E. Wilkins, *Biosens. Bioelectron.* **14**(7), 599–624 (1999). doi:[10.1016/S0956-5663\(99\)00039-1](https://doi.org/10.1016/S0956-5663(99)00039-1)
10. M.S. Kim, Y.R. Chen, P.M. Mehl, *Trans. ASAE* **44**, 721–729 (2001)
11. B. Cho, Y.R. Chen, M.S. Kim, *Comput. Electron. Agric.* **57**(2), 177–189 (2007). doi:[10.1016/j.compag.2007.03.008](https://doi.org/10.1016/j.compag.2007.03.008)
12. M.S. Kim, A.M. Lefcourt, Y.R. Chen, T. Yang, *J. Food Eng.* **71**(1), 85–91 (2005). doi:[10.1016/j.jfoodeng.2004.10.022](https://doi.org/10.1016/j.jfoodeng.2004.10.022)
13. M.S. Kim, Y.R. Chen, B.K. Cho, K. Chao, C. Yang, A.M. Lefcourt, D. Chan, *Sens. Instrum. Food Qual. Saf.* **1**(2), 151–159 (2007). doi:[10.1007/s11694-007-9017-x](https://doi.org/10.1007/s11694-007-9017-x)
14. M.S. Kim, A.M. Lefcourt, Y.R. Chen, *Appl. Opt.* **42**(19), 3927–3934 (2003). doi:[10.1364/AO.42.003927](https://doi.org/10.1364/AO.42.003927)
15. J.H. Ryu, H. Kim, J.F. Frank, L.R. Beuchat, *Lett. Appl. Microbiol.* **39**(4), 359–362 (2004). doi:[10.1111/j.1472-765X.2004.01591.x](https://doi.org/10.1111/j.1472-765X.2004.01591.x)
16. R.A. Pimentel, *Morphometrics—The Multivariate Analysis of Biological Data* (Kendall/Hunt, Dubuque, 1979)
17. K. Scher, U. Romling, S. Yaron, *Appl. Environ. Microbiol.* **71**(3), 1163–1168 (2005). doi:[10.1128/AEM.71.3.1163-1168.2005](https://doi.org/10.1128/AEM.71.3.1163-1168.2005)
18. X. Zogaj, M. Nimtz, M. Rohde, W. Bokranz, U. Romling, *Mol. Microbiol.* **39**(6), 1452–1463 (2001). doi:[10.1046/j.1365-2958.2001.02337.x](https://doi.org/10.1046/j.1365-2958.2001.02337.x)
19. A. Reisner, K.A. Krogfelt, B.M. Klein, E.L. Zechner, S. Molin, *J. Bacteriol.* **188**(10), 3572–3581 (2006). doi:[10.1128/JB.188.10.3572-3581.2006](https://doi.org/10.1128/JB.188.10.3572-3581.2006)
20. P. Leonard, S. Hearty, J. Brennan, L. Dunne, J. Quinn, T. Chakraborty, R. O’Kennedy, *Enzyme Microb. Technol.* **32**(1), 3–13 (2003). doi:[10.1016/S0141-0229\(02\)00232-6](https://doi.org/10.1016/S0141-0229(02)00232-6)
21. O. Lazcka, F.J.D. Campo, F.X. Munoz, *Biosens. Bioelectron.* **22**(7), 1205–1217 (2007). doi:[10.1016/j.bios.2006.06.036](https://doi.org/10.1016/j.bios.2006.06.036)